

Quasiepitaxial growth of a monoclinic phase on UO_2 single crystals upon leaching in H_2O

L. Nowicki* and A. Turoś†

Soltan Institute for Nuclear Studies, Hoza 69, PL-00-681 Warsaw, Poland

C. Choffel, F. Garrido, and L. Thomé

Centre de Spectrométrie Nucléaire et de Spectrométrie de Masse, IN2P3-CNRS, Bât. 108, F-91405 Orsay, France

J. Gaca and M. Wójcik

Institute of Electronic Materials Technology, Wolczynska 133, PL-01-919 Warsaw, Poland

Hj. Matzke

European Commission, JRC, Institute for Transuranium Elements, P.B. 2340, D-76125 Karlsruhe, Germany

(Received 16 October 1996; revised manuscript received 21 February 1997)

Surface oxidation of (110)-oriented UO_2 single crystals leached in demineralized water at 180 °C for 24 h has been studied by means of the backscattering/channeling technique. The O sublattice was analyzed using the $^{16}\text{O}(^4\text{He}, ^4\text{He})^{16}\text{O}$ resonance occurring at 3045 keV. Quasiepitaxial growth of an oxidized surface layer was observed and attributed to the phase transformation from the cubic UO_2 to a monoclinic UO_r phase with $r = 2.28 \pm 0.05$. X-ray diffractometry was also used to study the orientation of (110) atomic planes of the transformed layer with respect to the bulk crystal and to measure the change of the (110) interplane distance. A simple geometrical model of the quasiepitaxial growth is proposed and the distortion of the UO_2 cubic elementary cell due to the incorporation of surplus oxygen atoms is determined. Monte Carlo simulations of channeling data confirm the model and provide indications about atom location. The observed monoclinic phase is compared with other phases of uranium oxides. [S0163-1829(97)00326-3]

I. INTRODUCTION

Nuclear waste management is one of the most important technical and ecological problems involved in the use of nuclear power reactors. In the direct storage scenario the spent fuel is stored in safe, deep geological repositories. However, an accidental contact with water can lead to the loss of integrity of the waste form, which in turn would produce leaching of radioactive material and its transport to the geosphere with the groundwater. Since today's nuclear fuel is UO_2 , the study of the corrosion mechanism of this material in aqueous solutions is of primary interest. Although a considerable effort has been spent to investigate this problem, there still remain questions about phase relationships and structural transformations in the uranium-oxygen-water system.¹

Uranium oxides present an almost unique group of chemical compounds because of the complexity of their phase relationships and because of the wide range of nonstoichiometric stability. Detailed crystallographic data of U_xO_y structures were presented in Table I of Ref. 1 and also in a shortened form in Table I of Ref. 2. The crystalline structures of uranium oxides vary from the fluorite structure and its distorted configurations (UO_2 , U_4O_9 , U_3O_7 , and $\gamma\text{-U}_2\text{O}_5$) to so-called layered structures in which mixed U-O planes are linked by straight U-O-U uranyl bonds. Some U_2O_5 phases and other higher oxide compounds (e.g., U_3O_8) up to UO_3 belong to this group. According to our previous studies^{3,4} it is known that leaching in water produces substantial changes in surface regions of UO_2 single crystals. These effects are due to the formation of higher oxides on the surface. Accord-

ing to Refs. 5–8, where water corrosion of polycrystalline UO_2 was studied, the formation of a $\text{UO}_{2.33}$ layer is an important stage of the oxidation process. Using x-ray diffractometry (XRD) the produced layer was identified as U_3O_7 .⁸ The formation of U_4O_9 , which is the common intermediate state in dry UO_2 oxidation,⁹ has also been reported for leaching of unirradiated UO_2 [e.g., in water at 340 °C, 15 MPa (Ref. 10)], and it is commonly found in leached UO_2 irradiated to a higher burnup. Thus, an effort should be made to determine in greater detail the phases produced in wet oxidation. The incorporation of oxygen into a UO_2 cubic elementary cell induces some modifications of the crystalline structure. However, all four reported U_3O_7 phases belong to the same family of distorted fluorite since their elementary cells (or subcells of larger structures) differ only slightly from the UO_2 elementary cube: three of them (α , β and γ) are tetragonal (with the c/a ratio very close to 1) and the fourth one (δ) is monoclinic ($\beta=90.29^\circ$ and $c/a \sim 1$). Except the particular case of $\gamma\text{-U}_2\text{O}_5$, the $r=2.33$ composition is an effective limit stage of crystalline structures based on the fluorite UO_2 (cubic) cell.⁶ In the presence of water at the stage of $r=2.33$ the onset of an oxidative dissolution process occurs. For air oxidation, further incorporation of oxygen induces a structural transformation from the fluorite-type to the layered phases. The final product of this process is a U_3O_8 compound (e.g., Refs. 11, 12), which, however, is very rarely obtained in aqueous chemical reactions.

The aim of this work was to study the structural changes in the surface region of UO_2 single crystals subjected to leaching in water. The specific condition of oxidative corrosion in demineralized water at 180 °C for 24 h was used.

Single crystals were selected in order to use the Rutherford backscattering/channeling technique for analysis. The present study is aimed thus at providing basic data for well controlled leaching conditions. Real spent UO_2 fuel is polycrystalline, contains dissolved fission products, and precipitates and bubbles of insoluble fission products; in addition, radiolysis effects occur in the leaching solution. In the case of UO_2 single crystals (as for spent fuel) two main features were of interest: (i) concentration of oxygen and its depth distribution, and (ii) transformations of the crystalline structure induced by incorporation of additional oxygen atoms. As a main technique to address these questions the backscattering/channeling method was used. The XRD was implemented as an additional technique to study the orientation of (110) planes in the transformed layer and changes of their mutual distances in respect to the crystal bulk. In the previous study by Tuross *et al.*⁴ on leached (110)-oriented UO_2 single crystals an angular shift of 0.8° of the [110] axis between the leached region and the bulk crystal was observed and was interpreted as a tetragonal distortion of the surface layer structure. The present work goes far beyond that study. A detailed investigation was performed on the parameters of the elementary cell of the oxidized region in order to elucidate the mechanism of the phase transformation produced under oxidative leaching in demineralized water (180 °C, 24 h).

II. EXPERIMENT

The samples were (110)-oriented UO_2 single crystals polished with a diamond paste and heated at 1500 °C in an $\text{Ar}/(8\%)\text{H}_2$ atmosphere in order to anneal mechanical damage.¹³ The stoichiometric composition was determined by gravimetry and confirmed by oxygen potential measurements. The quality of the single crystals was attested by a channeling χ_{\min} value of 0.015 measured before subsequent treatments. Leaching was made in water of pH=6 at 180 °C during 24 h in an autoclave at the Institute for Transuranium Elements at Karlsruhe.

The He-ion backscattering/channeling technique^{14,15} was used for determination of thickness, composition, and crystalline structure of the leached layers. Channeling experiments were performed at the ARAMIS facility¹⁶ of the CSNSM Orsay with a ^4He beam of 3070 keV to take advantage of the $^{16}\text{O}(^4\text{He}, ^4\text{He})^{16}\text{O}$ resonant scattering occurring at 3045 keV.¹⁷ The used energy of the incident ions enabled simultaneous analysis of backscattering yields from U and O atoms. Random backscattering spectra were recorded using a rotating random procedure with a tilt angle of 5° in order to avoid channeling effects. Angular scans were performed by means of a computer-controlled four-motor goniometer (two axis of rotation and x - y translation) of angular resolution better than 0.05° .¹⁸ Scattered ^4He ions were registered by a silicon surface barrier detector located at 165° . The energy resolution of the experimental setup was 15 keV, corresponding to a depth resolution of about 10 nm.

The XRD analysis was performed at IEMT Warsaw by means of a high-resolution diffractometer by measuring the $(\theta - \omega/2\theta)$ scans. $\text{Cu } K\alpha_1$ radiation was applied. To ensure negligibly small divergence of the primary beam a line focus and a Ge (400) monochromator were used. Care was taken to

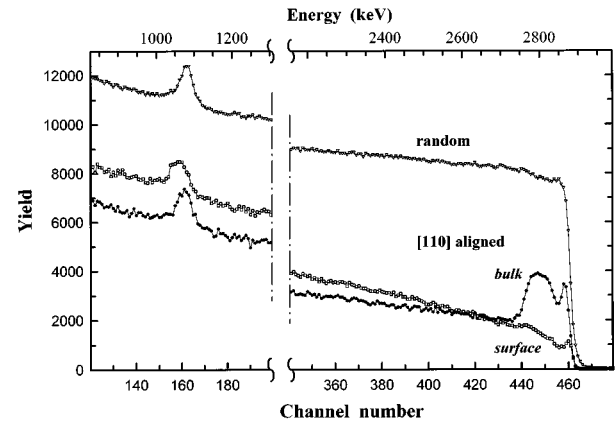


FIG. 1. Random and aligned backscattering spectra for the [110] UO_2 single crystal leached in water. The spectra labeled *bulk* and *surface* are recorded for the crystal aligned with the [110] axis of the bulk crystal and the transformed layer, respectively.

optimize the detection resolution by using a second Ge (200) monochromator and by using precise slits in front of the detector. A counter aperture on the order of 10^{-4} and a chromatic dispersion $\Delta\lambda/\lambda < 0.005$ were attained. The penetration depth of the XRD method in UO_2 is about 1 μm .

III. RESULTS

A. Composition of oxidized layer

A random backscattering spectrum for the leached UO_2 single crystal is shown in Fig. 1. The drawing was separated into two parts: (i) a high-energy portion (between channels 340 and 460) which is due to backscattering on the U atoms situated in the near-surface region, i.e., up to a depth of ~ 800 nm of the sample; (ii) a low-energy portion showing the peak of oxygen resonant scattering. The spectrum exhibits a clear deficiency in the U backscattering yield between channels 442 and 460 corresponding to a depth interval from 0 to 140 nm. This region of the spectrum can be seen in detail in the upper part of Fig. 2 where the spectrum measured for the leached sample is compared to the spectrum measured for a virgin crystal. The observed deficiency is caused by the change of the energy loss of probing He ions due to the incorporation of additional O atoms. The oxygen resonance peak around channel 162 is registered on a high background produced (almost on the whole) by scattering on uranium atoms. Since the energy of incident ions reaches the resonant value of 3045 keV at the depth of 60 nm the peak area is a measure of the oxygen content at this depth. Comparison of the oxygen resonant peaks measured for the leached crystal and the one for the virgin crystal made in the bottom part of Fig. 2 clearly demonstrates an increase of oxygen content in the leached sample.

To analyze the random spectrum in a quantitative manner, the RUMP code^{19,20} was used. The fits to the experimental data are presented in Fig. 2 by the solid lines. The best fit to the data for the leached sample was obtained assuming a surface layer of composition $\text{UO}_{2.28}$ and of thickness $\sim 1.0 \times 10^{18}$ atoms/cm² (~ 140 nm). Since the crystalline structure influences the backscattering yield also a few degrees off the axis²¹ we estimate that the systematic error affecting the

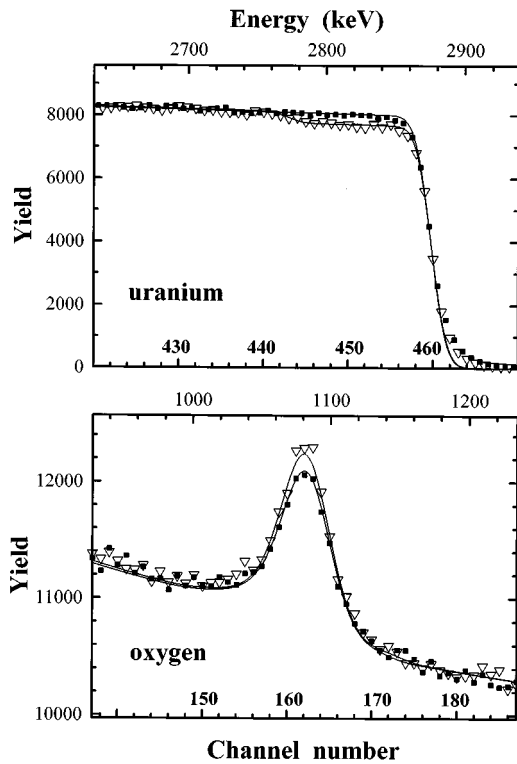


FIG. 2. Two parts of random backscattering spectra recorded with 3070 keV ^4He ions for virgin (circles) and leached (triangles) UO_2 single crystals. The upper part shows the backscattering on uranium atoms from the 0–500 nm depth interval. The bottom part presents the oxygen resonant peak. The solid line shows the spectra calculated with the RUMP code (Ref. 19).

value $r=2.28$ is less than 0.05. The high-energy part of the random spectrum reveals also that the composition of the oxidized layer is constant at least up to a depth of 115 nm.

B. Channeling analysis

In the standard angular scanning procedure, the collected counts are summed up over an energy region corresponding to a chosen depth interval. In the channeling measurements performed here, two regions were chosen: the first one labeled *bulk* (between channels 399 and 429) corresponded to a 230–440 nm depth region, the second one labeled *surface* (between channels 447 and 457), corresponded to a shallower depth interval from 25 to 95 nm. In both cases the yields in these regions are due to the scattering from uranium atoms. The angular scan performed along the (001) plane through the [110] axis revealed that for both depth regions an axial minimum was observed. However, these minima do not coincide, the surface dip minimum is displaced by 0.75° with respect to the bulk one. The aligned spectra measured at these angular positions which correspond to the observed minima are shown in Fig. 1. The aligned spectra shown here are labeled *bulk* and *surface* since they correspond to [110] axes for the bulk crystal and for the oxidized layer, respectively.

The strong difference in the shape observed for the *bulk* and *surface* spectra indicates that the leaching process has induced a crystallographic transformation in the surface re-

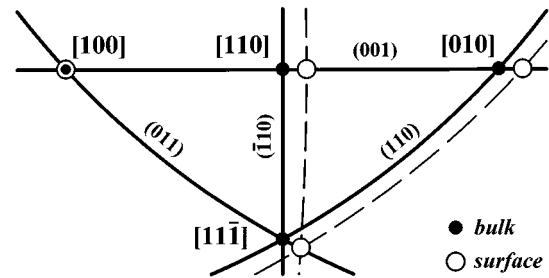


FIG. 3. Simplified [110] stereographic projection of the leached UO_2 single crystal. Circles denote localized axes. Positions of planes are shown by solid lines for the bulk crystal and dashed lines for the transformed layer.

gion of the UO_2 sample. The dechanneling level obtained in both aligned spectra is significantly higher than that obtained for the virgin crystal ($\chi_{\min}=0.015$). A very large surface peak and a rapid increase of the backscattering yield around channel 450 appearing in the *bulk* spectrum are due to the strong dechanneling produced by the misalignment of the incident beam in the crystal structure of the transformed layer. At greater depth, i.e., about 200 nm (channel 435) the backscattering yield sharply decreases since the analyzing ions are now well channeled in the unperturbed bulk crystal. The shape of the aligned *surface* spectrum can be understood by considering that the progressive dechanneling observed between channels 440 and 455 is due to the displacement of U atoms induced by the incorporation of additional O atoms. As a matter of fact, the effect of displaced O atoms on dechanneling is small or even negligible.²²

The structural analysis was performed by recording angular scans across four low-index axes: [100], [110], [010], and [11 $\bar{1}$] presented in a simplified [110] stereographic projection shown in Fig. 3. In this stereogram full circles and solid lines hold for the major axes and planes of the cubic crystal structure (*bulk* region), while open circles and dashed lines schematize corresponding axes and planes found for the transformed layer (*surface* region). As can be seen for only one ([100]) of these four axes the directions corresponding for *bulk* and *surface* regions are the same, while some angular shifts were observed in the case of the other three axes. Further, measures of these angular shifts between crystallographic axes of the surface and the bulk crystalline structures will be called declinations (on a far analogy to the term ‘magnetic declination’ used in geophysics). In order to elucidate details of these intrinsic misalignments angular scans measured along the (001) and (011) planes were analyzed. These scans are shown in Figs. 4 and 5. Apart from U scans (for *bulk* and *surface* regions) there are also represented the oxygen O scans measured at the depth of 60 nm. The oxygen yield was obtained by calculating the O-peak area after due subtraction of a continuous uranium background.

As it can be seen in Figs. 4 and 5 the angular positions of uranium dips for the [100] axis and both depth regions (*bulk* and *surface*) coincide within the experimental accuracy. On the other hand, the surface uranium dips for the other two axes in this plane: [110] and [010], are shifted from their original positions in the cubic structure by 0.75° . The bulk U scans for the [110] and [010] axes are split into two dips.

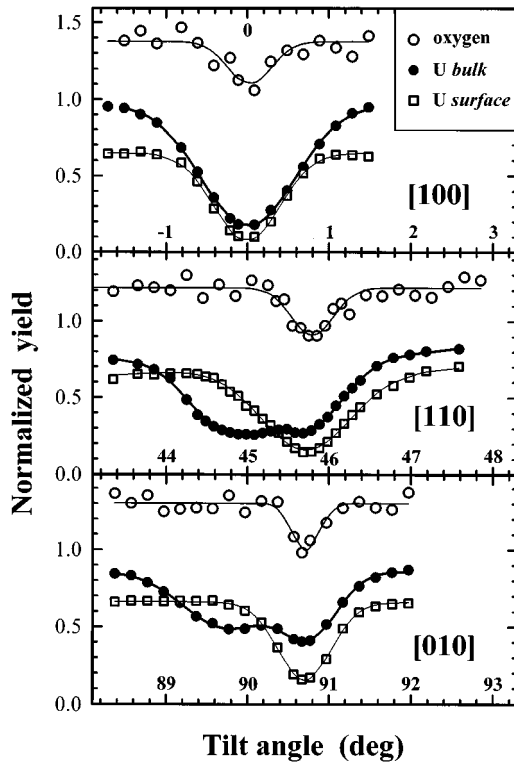


FIG. 4. Angular scans across various axes along the (001) plane for *bulk* and *surface* regions for the leached UO_2 single crystal. The tilt angle is defined as the angle with respect to the $[100]$ direction.

Their minima correspond to both (*surface* and *bulk*) directions of the channel. This result is due to the fact that particles channeled in the surface layer more easily enter into bulk channels than those that are not channeled in the surface region. This interpretation is supported by results of Monte Carlo simulations presented in Sec. IV C. A similar declination was also observed between bulk and surface $[11\bar{1}]$ axes in the (011) plane (cf. Fig. 5). The angle between $[100]$ and $[11\bar{1}]$ axes for the cubic structure is 54.74° ; in contrast, a value larger by about 0.65° was observed.

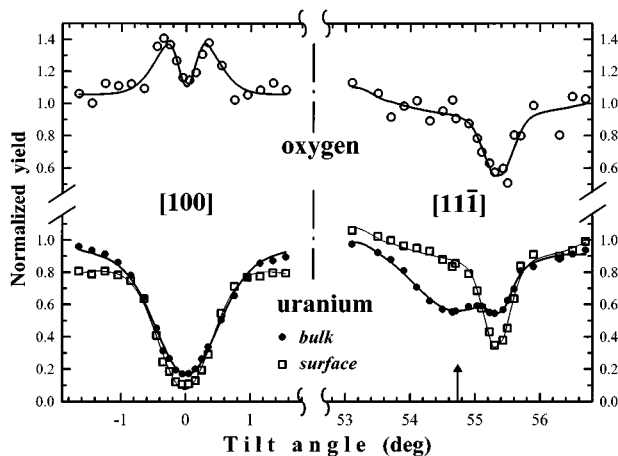


FIG. 5. Angular scans across the $[100]$ and $[11\bar{1}]$ axes along the (011) plane for the leached UO_2 single crystal. The arrow shows the position of the $[11\bar{1}]$ axis in a cubic structure. The tilt angle is defined as the angle with respect to the $[100]$ direction.

A common feature of the various O scans presented in Figs. 4 and 5 is that the oxygen dips for the four axes coincide with the corresponding *surface* U dips. This observation is consistent with the interpretation of the U scans, since the O scans were always recorded for the transformed layer. Moreover, two important details have to be noted. The first one is a planar flux peaking observed in the (001) plane, i.e., the normalized yield outside the axial minimum reaches a value close to 1.35 instead of a typical value of 0.3–0.6. This effect is due to the large difference between the atomic numbers of U and O atoms: O atoms can be considered as perturbing impurities in the U sublattice which is decisive for the channeling flux formation. The second feature is that the oxygen dips are very shallow for the three axes in the (001) plane. Their minima are close to 1 (i.e., they correspond to the random value) or, in the case of the $[100]$ axis, they even slightly exceed 1. This finding indicates an important transformation of the O sublattice that is produced by the incorporation of surplus O atoms upon leaching.

The observed declination between the three low index axes and the directions fixed by the cubic structure of the bulk crystal reveals that the elementary cell of the oxidized phase is substantially distorted with respect to the UO_2 cubic elementary cell. Table I summarizes the angles between the crystal axes in the case of a cubic structure and those measured for the bulk crystal and the transformed layer.

C. XRD analysis

The samples were investigated by means of reciprocal space mapping in the vicinity of the (220) bulk reflection. The applied method made it possible to determine the interplanar spacing of (110) planes as well as their mutual misorientation between the bulk and the transformed layer. Figure 6 presents the contour map of the analyzed region of the reciprocal space. The equal intensity lines are plotted in a logarithmic scale. The measurements were carried out with a step of 0.0032° for the 2θ angle and with a step of 0.0256° for the ω angle. The 2θ and ω angles correspond to q_{110} and q_{001} reciprocal-space vectors, respectively. The center of gravity of the main reflection, i.e., the bulk reciprocal-lattice point is located at the origin of the map $(q_{110}, q_{001}) = (0, 0)$. The reflection from the transformed layer can be found as the smaller peak around $(q_{110}, q_{001}) = (6.995 \times 10^{-2} \text{ nm}^{-1}, 0.001 \times 10^{-2} \text{ nm}^{-1})$.

The noteworthy feature of this map is that the centers of gravity of both peaks lie along the $q_{001} = 0$ line. Thus, the

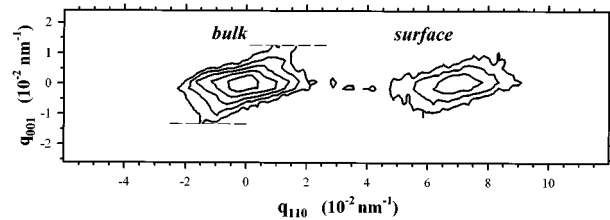


FIG. 6. Contour plot of the XRD reciprocal space map for a leached UO_2 sample near the (220) reflection. Equal intensity lines were drawn in a logarithmic scale; they differ by a factor of 3.16. The higher peak corresponds to the UO_2 cubic substrate (*bulk*), the lower one to the transformed layer (*surface*).

TABLE I. Angles between low-index axes for the ideal cubic structure and for the bulk and transformed layer of the leached crystal.

Symbol	Directions forming the angle	Angle for ideal cubic structure (deg)	Measured angle (deg)	
			Bulk	Transformed layer
φ	[100] [110]	45.00	45.00	45.75
γ	[100] [010]	90.00	89.95	90.75
ψ	[100] [11 $\bar{1}$]	54.74	54.70	55.35
δ	[110] [11 $\bar{1}$]	35.26	35.25	35.45

(110) planes of the transformed layer are parallel to the bulk planes. The (110) interplanar spacing in the transformed layer can be calculated from the distance between the peaks along the q_{110} direction. From this measurement an interplanar spacing of 191.26 pm was deduced which is by 2.13 pm smaller than that for the bulk crystal. As compared to what can be expected for a perfect crystal both peaks are rather wide. Although a quantitative analysis of this effect is hardly possible, some general remarks can be formulated. The broadening of peaks along the q_{110} direction indicates that large amounts of defects are incorporated in both regions. The width of the peaks in the perpendicular direction can be attributed to the mosaic spread of the crystal. One significant observation is that since the widths of both peaks in either direction are roughly the same, neither additional defects nor mosaic spread were introduced upon transformation. It seems to indicate that the transformed layer “inherited” the substrate structure without important modifications.

IV. DISCUSSION

The U_xO_y phases are often observed with a nonstoichiometric composition^{1,23} and exhibit polymorphism. Thus the value of r (or the O/U ratio) for a given uranium oxide does not allow us to identify the phase. The structure and dimensions of the elementary cell and consequently the lattice location of atoms, are of prime importance for this identification. In the following, a simple geometrical model describing the link between transformed and nontransformed regions of the crystal is proposed. Then, elementary cell parameters of the phase observed in the transformed region are deduced from the channeling and XRD data reported in the previous section.

A. Geometrical model of the transformed layer

Figure 7 displays a model of the structure formed at the surface of a (110)-oriented UO_2 single crystal upon leaching. The cubic (fluorite type) structure is shown in the bottom part of the drawing (*bulk*), whereas the distorted phase is shown in the upper part (*surface*). The comparison between the two structures shows that the [100] axes are exactly aligned in both parts of the crystal, while a declination of about 0.75° between bulk and surface regions for the other main axial directions ([110] and [010]) exists. This description also includes the existence of a transition layer since one can expect that the stress due to the lattice mismatch between both structures is relaxed over a certain depth interval. Thus,

the geometrical model is parametrized by the thickness d_m of the transformed layer, the thickness d_t of the transition layer and the declination ϵ .

The transformed oxidized layer can be considered as quasiepitaxial since it was grown on the crystal with conservation of the direction of one of the low-index crystal axes. The formation of the transformed layer presents a strong analogy with a solid-state epitaxy process. However, it should be pointed out that the formation of the transformed layer does not result as a growth of a structure on the crystalline substrate, but from an ingrowth towards the crystal bulk.

B. Elementary cell of the transformed layer structure

The results of channeling and XRD experiments presented above enable the determination of the shape of the elementary cell of the transformed layer. Figure 8 shows such a cell and defines the angles. The fact that the (001) planes of the transformed layer and of the bulk crystal coincide with each other allows one to conclude that angles α and β are unaffected by the transformation, i.e., they are equal to 90° . One can calculate the b/a ratio as

$$\frac{b}{a} = \frac{\sin \varphi}{\sin(\gamma - \varphi)} = 1.0130 \pm 0.0015. \quad (1)$$

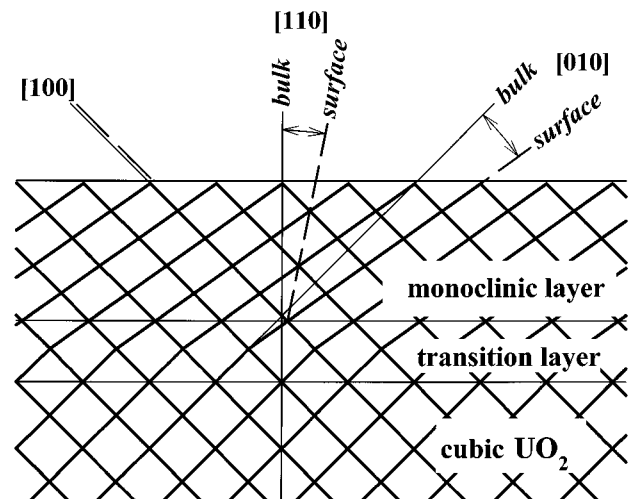


FIG. 7. Structural model of the quasiepitaxial monoclinic surface layer grown on the cubic UO_2 structure.

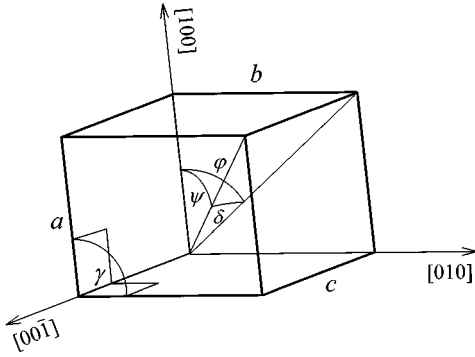


FIG. 8. Monoclinic elementary cell of the transformed layer structure.

On the other hand, since the (110) planes of the transformed layer and of the bulk crystal are parallel, the same parameter can be obtained by using the formula

$$\frac{b}{a} = \frac{\sin 45^\circ}{\sin(135^\circ - \gamma)} = 1.0134 \pm 0.0010. \quad (2)$$

The estimations of the errors in formulas (1) and (2) were calculated by taking into account the accuracy of 0.05° in the determination of the directions of the crystalline axes. The b/a ratios given by Eqs. (1) and (2) are equal within the limits of errors. This allows one to take $b/a = 1.0132 \pm 0.0010$ as a common result.

To determine the c/a ratio, the system of four experimentally measured angles (φ , γ , δ , and ψ) is used. By resolving a simple solid-geometry problem one can calculate this parameter by using two different formulas:

$$\frac{c}{a} = \frac{\sin \gamma \operatorname{tg} \delta}{\sin(\gamma - \varphi)} = 1.0068 \pm 0.0010 \quad (3)$$

and

$$\frac{c}{a} = \frac{1}{\cos \psi} \sqrt{\left[1 + 2 \frac{b}{a} \cos \gamma + \left(\frac{b}{a}\right)^2\right] \sin^2 \psi - \left(\frac{b}{a}\right)^2 \sin^2 \gamma} = 1.0059 \pm 0.0015. \quad (4)$$

They lead to $c/a = 1.0065 \pm 0.0010$.

Next, considering that the distance between the (110) planes of the transformed layer is reduced by 2.13 pm with respect to the bulk, the parameters of the elementary cell of the oxidized crystal were calculated. The following values were found: $a = 541.0$ pm, $b = 548.1$ pm, $c = 544.5$ pm, $\alpha = 90^\circ$, $\beta = 90^\circ$, $\gamma = 90.75^\circ$.

A previous preliminary analysis in which a (110) surface of leached UO_2 was also examined⁴ showed that one edge of the elementary cube was slightly shortened, which is in good agreement with the results presented here. However, the crystal structure transformation occurring on the (110) surface should not be called a ‘‘tetragonalization’’ (as it was in Ref. 4), since it consists in changes of both linear and angular parameters of the elementary cell. The word ‘‘monoclinization’’ is thus more appropriate. In the Monte Carlo simulations reported in Ref. 4, based on a tetragonalization model, a reduction of the edge a by 2.8% was assumed, correspond-

ing to a 0.8° declination of the [110] axis. In the present monoclinization model this reduction is smaller due to the observed increase of the angle γ .

C. Monte Carlo simulations

The above interpretation of the channeling spectra and of the angular scans are straightforward. Nevertheless, one can expect that Monte Carlo computer simulation of ion channeling can enrich our knowledge of the structure of the oxidized layer and its link with the crystal bulk. However, precise determination of the atomic positions is very difficult due to the complexity of the transformed structure. For instance, for closely related structure of $\beta\text{-U}_4\text{O}_{9-y}$ a $4a \times 4a \times 4a$ supercell containing 256 uranium and 572 oxygen atoms was proposed.^{24,25} Thus, the present description limits the aims of the simulations to the following items: (i) verification of the presented interpretation of the angular shifts, and (ii) modeling of the transition layer between the transformed and non-transformed regions. Moreover, to determine the extent to which the atomic locations in the transformed structure differ from the UO_2 fluorite atomic arrangement a simplified two-dimensional description of atomic locations is considered. Simulations of channeling data along the [110] direction are only presented.

The simulations were performed by using the MCCHASY code developed at SINS Warsaw. In this code the Monte Carlo method and the nuclear encounter probability approach^{26,27} were applied to calculate the backscattering yield of He ions passing through the crystalline structure in a direction close to a low index axis. In a simulation run several thousand trajectories of incoming He ions are calculated with the binary collision approximation. The crystal structure is treated as a sequence of monolayers and the interaction of the He ion with at least three closest atoms of each monolayer is taken into account. The scattering angle of a He ion in a single ion-atom collision is calculated assuming the universal Ziegler-Biersack-Littmark interaction potential²⁸ and by using the Gauss-Mehler quadratures.^{29,30} It was assumed that uranium and oxygen atoms vibrate isotropically with root-mean-square amplitudes $u_{\text{U}} = 7$ pm for uranium and $u_{\text{O}} = 10$ pm for oxygen. These values were calculated based on the known Debye-Waller factors for UO_2 .^{31,32} Channeling spectra for the structure described in the proposed geometrical model can be computed for different incident directions close to the main crystal axis. To obtain reasonably low statistical errors of an angular scan consisting of 30 directions, $\sim 10^5$ trajectories should be calculated. More details concerning the MCCHASY code will be published elsewhere.³³

To shed some light on lattice positions of atoms in the transformed structure it was assumed that uranium atoms in the [110] rows are displaced in such a way that in projection on the (110) plane they form a two-dimensional Gaussian distribution, parametrized by two dispersion parameters σ_x^{U} and σ_y^{U} which correspond to the directions [110] and [001], respectively. Moreover it was assumed that all oxygen atoms, i.e., matrix atoms as well as those incorporated during leaching, lie close to the matrix [110] rows and are also dispersed with a Gaussian distribution. In order to restrict the number of free parameters, an isotropic spread was assumed, which is parametrized by the dispersion σ^{O} . Thus, the pro-

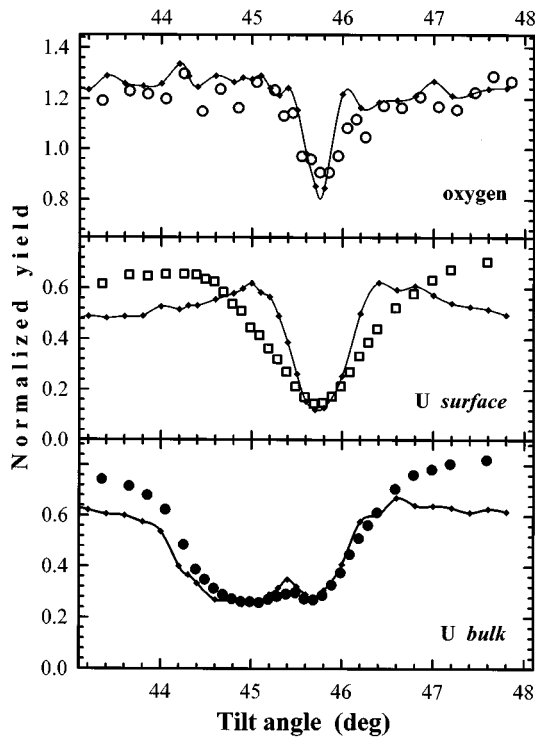


FIG. 9. Experimental angular scans (as shown in Fig. 4) measured along the (001) plane across the [110] axis compared to the results of Monte Carlo simulations.

posed model considers changes in both sublattices, although the general fluorite-type arrangement of atoms is preserved. Note that the spreading of the [110] atomic rows could be considered as a splitting of these rows into several new ones. Consequently, this model includes in a simplified way the models of the U_4O_9 and U_3O_7 structures postulated in previous works.^{24,34,35} The two-dimensional description of the atomic positions is sufficient since, although channeling angular scans are very sensitive to the atomic distribution on the transverse plane, they are almost independent of the displacements of atoms along the channeling direction.³⁶

During the fitting procedure the transition layer thickness d_t , the declination ϵ and the dispersions σ_x^U , σ_y^U and σ^O were adjusted in order to obtain best fits to the angular scans as well as to the channeling spectra for both *bulk* and *surface* directions. Figure 9 presents fits to angular scans calculated using the parameters: $d_t = 40$ nm, $\epsilon = 0.75^\circ$, $\sigma_x^U = 30$ pm, $\sigma_y^U = 17$ pm, and $\sigma^O = 24$ pm.

Although the calculated and experimental scans do not agree in all details, the double-dip shape of the *bulk* angular scan is quite well reproduced by the fitting procedure. This result confirms the formation of a monoclinic phase. The value of 0.75° found for the declination ϵ is in agreement with the previous estimation of the angle γ since $\gamma = 90.0^\circ + \epsilon$. The nonzero value of the d_t parameter means that the [110] channel (and also other channels except the [100] one) is curved, i.e., bent in the interface region, instead of being sharply broken. The difference between σ_x^U and σ_y^U means that displacements of uranium atoms are larger in the plane (001), i.e., in the plane of the monoclinic distortion, than in the perpendicular (110) plane. The observed differ-

ences between simulated and experimental angular scans, especially for the *U-surface* scan, are probably due to the simplified description of atomic displacements. Finally, one should note, that the fits to oxygen angular scans are less reliable than the uranium ones because of the much greater experimental uncertainties obtained for O data. Moreover, it was shown that the uranium part of channeling spectra is weekly sensitive to oxygen atoms located inside the channel.²²

D. Comparison with other uranium oxides

At least eight uranium oxide phases of composition r in the 2.24–2.50 region are described by elementary cells (or subcells of a larger structure) very close to the fluorite cubic elementary cell of UO_2 with $a_0 = 547$ pm. They are: three polymorphs called α -, β -, and γ - U_4O_9 , four polymorphs called α -, β -, γ -, and δ - U_3O_7 and one polymorph called γ - U_2O_5 . The γ - and δ - U_3O_7 phases are known also as $U_{16}O_{37}$ and U_8O_{19} oxides, respectively.¹ The phase observed in the transformed layer belongs to the same family, since its elementary cell parameters a , b , c are also very close to a_0 and its monoclinic distortion is small ($\gamma - 90^\circ = 0.75^\circ$). A comparison between the observed monoclinic phase and known uranium oxide phases (not only those listed above) is discussed below. First, the linear parameters of the elementary cell are compared, then the monoclinic distortion is discussed, and finally atomic displacements are considered.

Among the phases listed above the largest differences between linear parameters a, b, c of the elementary cell were found for the δ - U_3O_7 phase ($a = c = 537.8$ pm) with the ratio $b/a = 1.033$ (Ref. 37) and the β - U_3O_7 phase ($a = b = 536.3$ pm) with $c/a = 1.031$.^{38,39} For the observed monoclinic phase the ratio b/a is equal to 1.013, being the same as b/a found for γ - U_2O_5 ,⁴⁰ and close to the $(c/a)^{-1} = 1.014$ characterizing the α - U_3O_7 oxide.³⁸ The observed differences of cell edge lengths clearly distinguish the observed phase from the U_4O_9 polymorphs characterized by $a = b = c$.⁴¹

The question to be addressed is whether it is possible to identify the observed phase as one of the four monoclinic phases already established for uranium oxides, namely: δ - U_3O_7 ($c/a = 1$, $b/a = 1.034$, $\beta = 90.29^\circ$),³⁷ γ - U_2O_5 ($c/a = 1$, $b/a = 1.013$, $\beta = 90.49^\circ$),⁴⁰ γ - U_3O_8 ($c/a = 1.274$, $b/a = 0.895$, $\beta = 122.07^\circ$),⁴⁰ and β - UO_3 ($c/a = 0.378$, $b/a = 1.386$, $\beta = 99.03^\circ$).⁴² The last two compounds can be readily excluded. Both the shape of their elementary cells and their chemical compositions are considerably different from those obtained for the transformed region. The first two phases, i.e., δ - U_3O_7 and γ - U_2O_5 , are more similar to the phase formed during leaching, but none of them is identical to it. The values of the monoclinically distorted angle are: 90.29° and 90.49° for δ - U_3O_7 and γ - U_2O_5 , respectively, instead of 90.75° as found in the experiment.

Although the a and b parameters of the observed phase are equal to the corresponding parameters of γ - U_2O_5 , the shapes of their elementary cells are different. The γ - U_2O_5 (and also δ - U_3O_7) elementary cell is composed of parallelepipeds with the following structure: two rhombs with sides $a = c$ and four rectangles with a smaller value of a and a larger value of b . On the other hand, the elementary cell of the leached phase is a parallelepiped composed of two par-

allelograms with a shorter side a and a longer side b , two rectangles with a longer side b and a shorter side a , and two rectangles with a longer side b and a shorter side c . It should be pointed out that the observed monoclinic distortion affects the angle between the shortest edge a and the longest edge b of an elementary parallelepiped and not the angle between equal edges, as it is the case for the δ -U₃O₇ and γ -U₂O₅ phases. Although these two phases were produced only at high pressure (>400 MPa), their similarity to the observed phase was also considered. This is motivated by the fact that the external pressure can be superseded by the intrinsic strain induced by a quasiepitaxial ingrowth of the monoclinic structure inside the cubic substrate. Such a strain can also result in increase of the monoclinic distortion.

Although no monoclinic distortion was noticed for the U₄O₉ polymorphs one detail concerning these phases should be discussed. The high-temperature phase: γ -U₄O₉ and the middle temperature phase β -U₄O₉ are cubic. The β -U₄O₉ phase transforms to the third known polymorph α -U₄O₉ upon decreasing the temperature below 65 °C.^{41,43} During this transformation the linear parameters of the elementary cell remain almost unchanged, but all three angular parameters increase from 90.0° to 90.078° to form a triclinic structure of α -U₄O₉. This effect of a tiny deformation of the elementary cell shows that the structure of U₄O₉ reveals instability towards deformation of angles. The declination effect observed in this work can be considered as a manifestation of a similar instability.

For the majority of phases listed in the beginning of this section the atomic lattice locations of U and O atoms remain unknown, although it is generally accepted that the uranium sublattice is close to the fcc-type UO₂ fluorite structure. The most reliable data of atom locations were obtained for the β -U₄O₉ oxide by Bevan, Grey, and Willis by using the neutron-diffraction method.²⁴ Based on the proposed structural model small displacements of uranium atoms from their fcc lattice positions were determined. These displacements lead to a spreading of atomic rows. The “thickness” of the uranium $\langle 110 \rangle$ row disturbed in this way can be characterized by the standard deviations of x and y position coordinates corresponding to the $[\bar{1}10]$ and $[001]$ directions, respectively. As it was calculated both deviations amount to 7.7 pm. Since the standard deviations of Gaussian distributions used to fit the experimental data amount to $\sigma_x^U = 30$ pm and $\sigma_y^U = 17$ pm, then the uranium sublattice in the observed phase is disturbed to a higher extent than in the case of β -U₄O₉ crystals. Similar comparison can also be made for the oxygen sublattice. According to this model oxygen $[110]$ rows are much more widely spread than the uranium ones. The corresponding standard deviations of x and y coordinates are 30 pm, i.e., only slightly larger than the standard deviations used in the simulations. Thus, the oxygen sublattice in the observed monoclinical phase is disturbed to a similar extent as in a β -U₄O₉ crystal.

Finally, one detail concerning oxygen atoms positions should be noticed. As it can be seen in Figs. 4 and 5, the minimum of the $[11\bar{1}]$ oxygen dip is 0.55, i.e., it is much lower than the corresponding value measured for the other three axes. This fact indicates that a majority of oxygen atoms still occupy positions in mixed rows of the $\langle 111 \rangle$ type. It implies that the determined monoclinic phase can be considered as a transition state from the UO₂ to the α -U₃O₈ phase transformation. In this transformation part of oxygen atoms forms colinear -O-U-O- bonds along the $\langle 111 \rangle$ directions.²

V. CONCLUSIONS

A transformation from the cubic (fluorite) UO₂ structure to the monoclinic UO_{2.28±0.05} phase was observed as a result of 24 h aqueous oxidation of (110)-oriented UO₂ single crystals at a temperature of 180 °C. The ingrowth of the transformed layer into the UO₂ structure, where one of the crystalline axis ($[100]$) of the bulk crystal is conserved, has a quasiepitaxial character similar to a solid-state epitaxy. A peculiar feature of the observed transformation is the fact that the conserved axis is not normal to the crystal surface but it forms with the normal an angle of $\sim 45^\circ$.

Channeling experiments performed for four low-index axes combined with XRD measurements enabled us to determine the structure of the formed monoclinic phase as consisted of cells described by $a = 541.0$ pm, $b = 548.1$ pm, $c = 544.5$ pm, $\alpha = \beta = 90.0^\circ$, and $\gamma = 90.75^\circ$. The phase belongs to the family of polymorphic structures existing in the UO_{2.24}-UO_{2.50} region. It cannot be concluded whether the obtained a , b , and c lengths concern an elementary cell or a subcell of a larger structure.

Channeling angular scans revealed that incorporation of additional oxygen atoms into the UO₂ structure results not only in the monoclinic deformation of the elementary cells but also in displacements of uranium and matrix oxygen atoms from their lattice sites. By applying a simple two-dimensional model that involves spreading of the $[110]$ atomic rows it was estimated that uranium atoms are preferentially displaced in the (001) planes in contrast to perpendicular ($\bar{1}10$) planes. The magnitudes of these displacements are larger than those observed for β -U₄O₉ crystals.

ACKNOWLEDGMENTS

The authors are grateful to C. Clerc for her help in running the computer-controlled goniometer system, and to the ARAMIS staff for their assistance during experiments. They thank J. Jagielski and V. Rondinella for helpful discussions. This work was supported by a grant from the EDF company (France) and by the Collaboration between IN2P3 (France) and Polish Laboratories.

* Author to whom correspondence should be addressed. FAX: +48-22-6213829. Electronic address: lech@fuw.edu.pl

† Also at Institute of Electronic Materials Technology, Warsaw.

¹D. K. Smith, B. E. Scheetz, C. A. F. Anderson, and K. L. Smith, *Uranium* **1**, 79 (1982).

²G. C. Allen and N. R. Holmes, *J. Nucl. Mater.* **223**, 231 (1995).

³Hj. Matzke and A. Turos, *Solid State Ion.* **49**, 189 (1991).

⁴A. Turos, R. Falcone, A. Drigo, A. Sambo, L. Nowicki, N. Madi, J. Jagielski, and Hj. Matzke, *Nucl. Instrum. Methods Phys. Res. B* **118**, 659 (1996).

- ⁵P. D. W. Bottomley and M. Coquerelle, *Corros. Sci.* **35**, 386 (1993).
- ⁶H. Christensen, S. Sunder, and D. W. Schoesmith, *J. Alloys Compd.* **213/214**, 93 (1994).
- ⁷S. Sunder, D. W. Schoesmith, R. J. Lemire, M. G. Bailey, and G. J. Wallace, *Corros. Sci.* **32**, 373 (1991).
- ⁸P. Taylor, D. D. Wood, D. G. Owen, and G.-I. Park, *J. Nucl. Mater.* **183**, 105 (1991).
- ⁹S. R. Teixeira and K. Imakuma, *J. Nucl. Mater.* **178**, 33 (1991).
- ¹⁰K. Une, S. Kashibe, and K. Nogita, *J. Nucl. Mater.* **227**, 32 (1995).
- ¹¹P. Taylor, D. D. Wood, and A. M. Duclos, *J. Nucl. Mater.* **189**, 116 (1992).
- ¹²P. Taylor, D. D. Wood, and D. G. Owen, *J. Nucl. Mater.* **223**, 316 (1995).
- ¹³Hj. Matzke and A. Turos, *J. Nucl. Mater.* **114**, 349 (1983).
- ¹⁴L. C. Feldman, J. W. Mayer, and S. T. Picraux, *Materials Analysis by Ion Channeling* (Academic, New York, 1982).
- ¹⁵A. Turos, Hj. Matzke, J. Chaumont, and L. Thomé, *Nucl. Instrum. Methods Phys. Res. B* **66**, 280 (1992).
- ¹⁶E. Cottreau, J. Camplan, J. Chaumont, R. Meunier, and H. Bernas, *Nucl. Instrum. Methods Phys. Res. B* **45**, 293 (1990).
- ¹⁷W. De Coster, R. Brijs, J. Goemans, and W. Vandervorst, *Nucl. Instrum. Methods Phys. Res. B* **66**, 283 (1992).
- ¹⁸C. Clerc (unpublished).
- ¹⁹L. R. Doolittle, *Nucl. Instrum. Methods Phys. Res. B* **9**, 344 (1985).
- ²⁰Z. Y. Zhou, Y. Y. Zhou, Y. Zhang, W. D. Xu, G. Q. Zhao, J. Y. Tang, and F. J. Yang, *Nucl. Instrum. Methods Phys. Res. B* **100**, 524 (1995).
- ²¹A. Dygo, W. N. Lennard, I. V. Mitchell, and P. J. M. Smulders, *Nucl. Instrum. Methods Phys. Res. B* **84**, 23 (1994).
- ²²A. Turos, O. Meyer, L. Nowicki, J. Rimmel, and M. Wielunski, *Nucl. Instrum. Methods Phys. Res. B* **85**, 448 (1994).
- ²³Y. Saito, *J. Nucl. Mater.* **51**, 112 (1974).
- ²⁴D. J. M. Bevan, I. E. Grey, and B. T. M. Willis, *J. Solid State Chem.* **61**, 1 (1986).
- ²⁵B. T. M. Willis, *J. Chem. Soc. Faraday Trans. 2* **83**, 1073 (1987).
- ²⁶J. H. Barrett, *Phys. Rev. B* **3**, 1527 (1971).
- ²⁷P. J. M. Smulders and D. O. Boerma, *Nucl. Instrum. Methods Phys. Res. B* **29**, 471 (1987).
- ²⁸J. F. Ziegler, J. P. Biersack, and U. Littmark, *The Stopping and Range of Ions in Solids* (Pergamon, New York, 1985).
- ²⁹Z. Kopal, *Numerical Analysis* (Wiley, New York, 1961).
- ³⁰A. Dygo and A. Turos, *Radiat. Eff. Lett.* **85**, 237 (1985).
- ³¹G. Dolling, R. A. Cowley, and A. D. B. Woods, *Can. J. Phys.* **43**, 1397 (1965).
- ³²B. T. M. Willis, *Proc. R. Soc. London, Ser. A* **274**, 134 (1963); B. T. M. Willis and R. G. Hazell, *Acta Crystallogr. Sec. A* **36**, 582 (1980).
- ³³L. Nowicki *et al.* (unpublished).
- ³⁴N. Masaki and K. Doi, *Acta Crystallogr. Sec. B* **28**, 785 (1972).
- ³⁵G. C. Allen and P. A. Tempest, *J. Chem. Soc. Dalton Trans.* **1982**, 2169 (1982).
- ³⁶O. Mayer and A. Turos, *Mater. Sci. Rep.* **2**, 371 (1987).
- ³⁷H. R. Hoekstra, S. Siegel, and P. Charpin, *J. Inorg. Nucl. Chem.* **30**, 519 (1968).
- ³⁸F. Westrum and F. Grønvoold, *J. Phys. Chem. Solids* **23**, 39 (1962).
- ³⁹It is still a matter of discussion whether β - U_3O_7 and δ - U_3O_7 are really distinct phases. See Refs. 2 and 37.
- ⁴⁰H. R. Hoekstra, S. Siegel, and F. X. Gallagher, *J. Inorg. Nucl. Chem.* **32**, 3237 (1970).
- ⁴¹B. Belbeoch, J. C. Boivineau, and P. Perio, *J. Phys. Chem. Solids* **28**, 1267 (1967).
- ⁴²V. I. Spitsyn, A. N. Tsigunov, L. M. Kovba and E. V. Kuz'mincheva, *Dokl. Akad. Nauk SSSR* **204**, 640 (1972).
- ⁴³K. Naito, *J. Nucl. Mater.* **51**, 126 (1974).